Suphapimol *et al. Journal of Inflammation* (2025) 22:6
https://doi.org/10.1186/s12950-025-00431-3

Journal of Inflammation

RESEARCH Open Access

Alpha-1 antitrypsin reduces inflammation and vasculopathy in mice with oxygen-induced retinopathy

Varaporn Suphapimol[1], Yu-Han Liu[2], Sandro Prato[2], Alexander Karnowski[2], Charles Hardy[2], Adriana Baz Morelli[2], Abhirup Jayasimhan[1], Devy Deliyanti[1] and Jennifer L. Wilkinson-Berka[1,3*]

Abstract

Background Damage to the retinal vasculature is a major cause of vision loss and is influenced by a pro-inflammatory environment within retinal tissue. Alpha-1 antitrypsin (AAT) is a potent inhibitor of serine proteases and has anti-inflammatory properties. We hypothesised that AAT could reduce inflammation and vasculopathy in neovascular retinopathies including oxygen-induced retinopathy (OIR).

Methods Litters of C57BL/6J mice were randomised to develop OIR by exposure to high oxygen between postnatal days 7 to 12 resulting in vaso-obliteration (phase I OIR), and then room air from postnatal days 12 to 18 resulting in neovascularisation (phase II OIR). Control mice were exposed to room air. Separate cohorts of mice were administered control vehicle or human AAT (120 mg/kg) by intraperitoneal injection every second day in phase I or phase II OIR.

Results In phase I OIR, plasma levels of AAT were reduced compared to room air controls, and AAT treatment reduced vaso-obliteration. In phase II OIR, AAT treatment influenced inflammation by reducing the density of ionised calcium binding adaptor protein 1 + cells (microglia/macrophages) and modulating their cell process length and reducing mRNA levels of tumour necrosis factor and monocyte chemoattractant protein-1, but not interleukin-1b and interleukin-6 in retina. Furthermore, AAT treatment reduced retinal neovascularisation, gliosis, vascular endothelial growth factor mRNA and protein expression, and vascular leakage, compared to OIR controls.

Conclusions This research demonstrates the vasculo-protective actions of AAT, and thereby the potential of AAT as a therapeutic option for neovascular retinopathies.

Keywords Alpha-1 antitrypsin, Oxygen-induced retinopathy, Inflammation, Microglia, Neovascularisation, Vascular leakage

*Correspondence:
Jennifer L. Wilkinson-Berka
jennifer.wilkinsonberka@unimelb.edu.au
[1]Department of Anatomy and Physiology, School of Biomedical Sciences, The University of Melbourne, Parkville, VIC, Australia
[2]CSL Limited, Melbourne, VIC, Australia
[3]School of Biomedical Sciences, The University of Melbourne, Level 2, Medical Building 181, Grattan Street, Parkville, VIC 3010, Australia

Background

Neovascular retinopathies such as retinopathy of prematurity and proliferative diabetic retinopathy, are leading causes of vision loss and blindness in premature babies and the working population, respectively [1, 2]. They feature retinal neovascularisation and vascular permeability due to breakdown of the blood-retinal barrier, with both events involving the increased expression of vascular endothelial growth factor A (VEGFA) [3–5]. Indeed, the ocular delivery of anti-VEGF agents is a predominant treatment approach for proliferative diabetic retinopathy [5, 6] and emerging for children with retinopathy of prematurity [7]. Yet, anti-VEGF agents are not entirely protective in all patients with diabetic retinopathy [5] and there are safety concerns for retinopathy of prematurity including reduced circulating VEGFA levels leading to neurocognitive decline and pulmonary hypertension [8, 9]. This has led to the necessity to further understand the biological mechanisms underpinning the pathogenesis of neovascular retinopathies. An important mechanism is inflammation that contributes to retinal vascular disease through cytokines, chemokines, and other factors produced by certain immune cells [10–12]. These immune cell populations include microglia, macrophages, and CD8 + T cells that infiltrate the retina through a damaged blood-retinal barrier [10–12].

Alpha-1 antitrypsin (AAT) is a sialoglycoprotein encoded by the SERPINA1 gene that is mainly produced by liver hepatocytes and to a lesser extent pulmonary alveolar cells, tissue macrophages, blood monocytes, and neutrophils [13]. AAT is an inhibitor of serine proteases such as elastase, trypsin, thrombin, proteinase 3, and cathepsin G and acts to protect tissues from proteolytic tissue damage [13, 14]. Indeed, inherited genetic deficiency of AAT can result in liver disease and emphysema due to the loss of inhibition of serine proteases [15] with augmentation of AAT a recognised treatment approach [16]. In addition, AAT has immunomodulatory and anti-inflammatory properties through inhibition of serine proteases and possibly SERPIN activity independent mechanisms [17, 18]. Functioning as an acute phase protein, AAT released into the circulation can reach plasma levels three- to five-fold higher than normal in response to acute inflammation or infection. In addition to its anti-inflammatory properties, AAT has cytoprotective actions that are relevant to the retina [19–22].

In the current study we hypothesised that treatment with AAT would protect the vasculature in a murine model of retinopathy of prematurity known as oxygen-induced retinopathy (OIR).

Methods

Animals

All studies were approved by the University of Melbourne Animal Ethics Committee and adhered to the National Health and Medical Research Council of Australia's Guidelines for the Care and Use of Animals in Scientific Research. Pregnant C57BL/6J mice (JAX stock number 000664) were obtained from the Animal Resources Centre (Perth, Western Australia). All mice were given a standard mouse diet (#SF00-100, Specialty Feeds, Perth, Australia), and housed at a consistent temperature of 21–22 °C under a 12-hour light/dark cycle.

Oxygen-induced retinopathy

The OIR procedure occurs over two phases and was performed according to our previous publications [11, 23] and is a slightly modified version of the model established by Smith and colleagues [24]. Phase I OIR is characterized by extensive vaso-obliteration in the central retina due to the exposure of neonatal mice to hyperoxia from postnatal day (P) 7 to P12, that mimics when preterm infants receive supplemental oxygen to alleviate respiratory distress. Phase II OIR features neovascularization and vascular leakage due to the exposure of mice to room air for five days that induces retinal ischemia and the excessive production of vascular factors such as VEGFA [25]. In our study, litters of mice were randomised to control and OIR treatment groups. In phase I OIR, mouse pups and their nursing mothers were exposed to hyperoxia (75% oxygen) for 22 h per day between P7 to P12 in specialised chambers that were maintained by a Pro-ox 110 gas regulator (Biospherix, NY, USA) attached to medical-grade oxygen cylinders (Air Liquide, Victoria, Australia). Mice were then returned to room air until P18 (Fig. 1). Age-matched controls were housed in room air for the entirety of the study (21% oxygen).

To determine if AAT influenced the extent of vaso-obliteration that peaks in OIR during phase I, human AAT was administered to OIR mouse pups by intraperitoneal (IP) injection in a 20 µl volume every second day between P7 and P12 (Fig. 1). To determine if AAT influenced retinal neovascularization and inflammation, separate cohorts of mice were administered human AAT as described above and in phase II OIR between P12 to P18 (Fig. 1). Litters of OIR mice were randomised to be treated with vehicle (controls) or AAT (120 mg/kg in vehicle comprised of formulated buffer; 144 mM mannitol, 38 mM sodium chloride and 17 mM sodium phosphate, pH 7.0, CSL Limited, Victoria, Australia). Comparisons were made to OIR mice administered human serum albumin, HSA, 120 mg/kg) by IP injection and room air controls. The dose and timing of AAT treatment is based on previous studies [19–21]. OIR mice were included in the study if they had consistent body

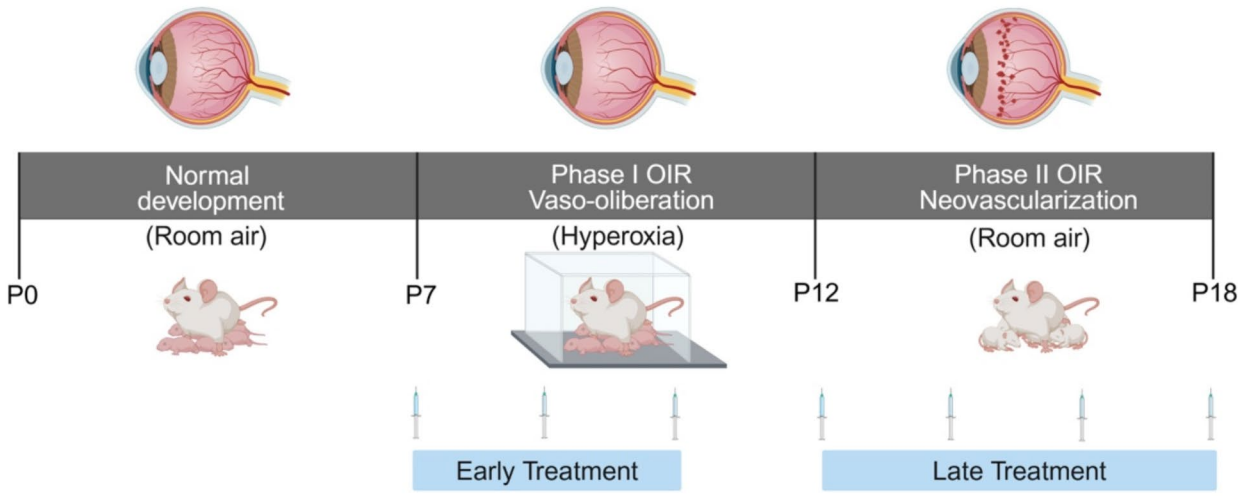

Fig. 1 Schematic diagram showing the OIR protocol and administration of AAT. P, postnatal day. Separate groups of OIR mice were treated with AAT in phase I OIR (P7 to P12) or phase II OIR (P12 to P18). Created with BioRender.com

weight gain in accordance with the established criteria for OIR studies [23]. As gender does not influence the development of OIR [26], both male and female mouse pups were studied. Mice were humanely killed at P12 or P18 with sodium pentobarbitone by IP injection (170 mg/ml, Virbac, Peakhurst, NSW, Australia).

Histological analysis of microglial/macrophage density in retina

Microglia resident within the retina proliferate and become activated in response to tissue injury [27]. The density of microglia can be determined by their expression of ionised calcium binding adaptor protein-1 (Iba1), although this marker also identifies macrophages. Here, the density of microglia/macrophages in the retina was evaluated with immunohistochemistry as previously reported [28, 29]. Three µm paraffin serial sections were obtained from one retina from each animal. Four sections of retina at least 60 µm apart were randomly selected and incubated with 10% normal goat serum (5425 S, Cell Signalling Technology, MA, USA). Sections were then incubated overnight at 4 °C with a rabbit anti-Iba1 antibody (1:1000, 019-19741, Wako, Tokyo, Japan). Sections were washed with 0.1 M phosphate buffered saline pH 7.4 (PBS), incubated for 1 h with biotin-conjugated goat anti-rabbit IgG (1:200, E0432, DakoCytomation), washed with PBS and then incubated with the Vectastain ABC standard kit (Vector Laboratories, Newark, CA, USA) for 30 min and liquid DAB + substrate chromagen system (Dakocytomation) for 15 s. Sections were counterstained with Mayer's Hematoxylin. For quantitation, 4 non-overlapping fields spanning the retina between the inner limiting membrane and inner plexiform layer, were captured at x400 magnification using a Nikon DS-Ri2 camera from each retina (Nikon Instruments Inc.). ImageJ software was used to set a threshold for immunolabeling which was applied to all fields. Data are presented as the percentage of Iba1 + cells per mm^2. Investigators were blinded to the experimental mouse groups.

To verify the effect of AAT on Iba1 + cells, immunolabelling for Iba1 was performed on flatmounted retina. Flatmounts were incubated for 1 h at room temperature with 10% normal goat serum in 0.3% Triton-100 at room temperature, and then overnight at 4 °C with anti-mouse Iba1 (1:100, Wako) dissolved in 1% normal goat serum, 0.3% Triton X-100 and PBS. Six successive 10-minute washes were performed with wash buffer (0.3% Triton X-100 in PBS). Retinas were incubated for 1.5 h at room temperature with anti-rabbit IgG Alexa Fluor® 548 (Molecular Probes, Eugene, OR, USA) dissolved in 1% normal goat serum and 0.3% Triton X-100. Retinas were washed 6 times and then incubated with FITC-conjugated isolectin (1: 100, L9381, Sigma) in 1% Triton X-100 to identify blood vessels. After washing, retinas were counterstained with DAPI (300 nM, Molecular Probes) to identify nuclei and mounted in fluorescent mounting medium (DakoCytomation). Retinal flatmounts were visualised with a Zeiss LSM800 scanning confocal microscope (Carl Zeiss AG, Oberkochen, Germany), with a 20x objective lens. Images were captured with Zen 2.3 software (Blue). Nine to twelve fields per retina were randomly selected from the ganglion cell layer to the inner plexiform layer. The density of Iba-1 + cells was quantitated by counting the number of Iba-1 + cells per field and presented as the number of Iba1 + cells per mm^2.

Quantitation of Iba1 + cell process length in retina

The activation of microglia can be visualised by the shortening of their cell processes [30]. Retinal flatmounts were prepared as described above and cell process length

was measured from the centre of the cell soma to the process tip using Image J software (v3.1, National Institutes of Health, Bethesda, WA, USA) in cells located in the ganglion cell layer and inner plexiform layer. The primary process of each Iba1 + cell was measured as previously reported [23]. Data are presented as the cell process length (μm) of Iba1 + cells.

Flow cytometry analysis for microglia and macrophages in retina

To further evaluate retinal microglia and macrophages, retinas were prepared for flow cytometry according to previous methods [11, 23]. Retinas were freshly dissected in Dulbecco's phosphate buffer saline containing calcium and magnesium (D-PBS with $Ca2^{+}/Mg^{+}$, #14040182, Thermo Fisher Scientific) supplemented with 0.5% bovine serum albumin and immediately processed for enzymatic digestion with a commercially available kit (Neural Tissue Dissociation kit #130-094-802, Miltenyi Biotec, NSW, Australia) according to the manufacturer's instructions for retinal tissues. Retinas were washed with 6 ml of D-PBS with $Ca2^{+}/Mg^{+}$ before transferring to a gentleMACS C tube (#130-096-334, Miltenyi Biotec) containing enzyme mixes from the kit for enzymatic digestion. Homogenization was performed using an automated dissociator (GentleMACS Octo Dissociator with Heaters, # 130-096-427, Miltenyi Biotec) according to the manufacturer's instructions for neuronal tissues. Digested retinas were further homogenised with gentle trituration with a 1 ml pipette. After dissociation, retinal homogenates were washed with 6 ml of D-PBS with $Ca2^{+}/Mg^{+}$ and 0.5% BSA and filtered twice through a 70 mm strainer (BD Biosciences, San Jose, CA, USA). Cells were spun down at 300 g for 10 min at room temperature and suspended in 1 ml D-PBS with $Ca2^{+}/Mg^{+}$ supplemented with 0.5% bovine serum albumin for cell counting using an automated counter (Countess II FL, Thermo Fisher Scientific). One and a half million retinal cells were incubated in D-PBS without $Ca2^{+}/Mg^{+}$ (#14190250, Thermo Fisher Scientific) containing CD16/CD32 antibodies (Mouse BD Fc Block, #553142) to block non-specific binding and a dead cell stain (Aqua, #L34957, Thermo Fisher Scientific) to exclude dead cells. Cells were washed twice with FACS buffer and further incubated with an antibody cocktail consisting of CD45 BV786 (#564225), and CD11b AF700 (#557960) antibodies for 45 min at 4 °C. Flow cytometry was performed using a Fortessa X-20 (BD Biosciences) with at least 100,000 events. Cell viability was 95.84 ± 4.51% ($n = 47$ from 4 independent experiments). FlowJo software (v 10.8.1, Tree Star, Inc., OR, USA) was used for data analysis. Unless otherwise specified, all products were purchased from BD Biosciences.

Quantitative PCR of retina

We utilised a previously published method [11, 23, 28], whereby total RNA was isolated from single retina using the RNeasy mini kit (Qiagen, Doncaster, VIC, Australia), and then 1 μg of RNA was subjected to DNase treatment (DNA-free kit, Ambion, Carlsbad, CA, USA) and reverse transcription (First Strand cDNA synthesis kit, Roche, Switzerland). mRNA expression was normalised to 18s rRNA endogenous control and the relative fold difference in expression was calculated using the comparative 2- ΔΔCt method. The primer sequences for *Vegfa* are forward primer: 5'-AGCAGAAGTCCCATGAAGT GATC-3 and reverse primer: 5'—TCAATCGGACGGC AGTAGCT-3'. The primer sequences for tumor necrosis factor (*Tnf*) are, forward primer: 5'-GCCTATGTCT CAGCCTCTTCTC-3' and reverse primer: 5'-CACTT GGTGGTTTGCTACGA-3'. The primer sequences for monocyte chemoattract protein – 1 (*Mcp-1*) are, forward primer: 5'-CAGGTGTCCCAAAGAAGCTGTAG-3' and reverse primer: 5'-GGGTCAGCACAGACCTCTCTC T-3'. The primer sequences for interleukin *Il-1b* are, forward primer: 5'-GTTCCCATTAGACAACTGCACTAC A-3' and reverse primer: 5'-CCGACAGCACGAGGCTT TT-3'. The primer sequences for *Il-6* are, forward primer: 5'-ACAAAGCCAGAGTCCTTCAGAGA-3'and reverse primer: 5'-CTTCTGTGACTCCAGCTTATCTGTTA G-3'.

Analysis of vaso-obliteration and neovascularisation in retinal flatmounts

Retinal flatmounts were prepared as described previously [11, 23]. Eyes were enucleated and fixed in 4% paraformaldehyde in PBS for 30 min at room temperature. Retinal flatmounts were stained with fluorescein isothiocyanate-conjugated isolectin (FITC) GS-IB4 (L9381, Sigma, St Louis, MI, USA) or PBS only (negative control) and imaged using a Zeiss Axio (Carl Zeiss, Gottingen, Germany) microscope attached to a camera (AxioCam MRc, Carl Zeiss). Entire retinal montages were obtained using the tiling tool in the AxioObverser Software (v5.3, Carl Zeiss). ImageJ was used to quantitate vaso-obliteration and neovascularisation using the threshold tool. Mice from 2 to 3 different litters were evaluated at P12 and P18. Investigators were blinded to the experimental groups.

Histological analysis of Müller cells in retina

Müller cells are macroglia that extend across almost the entire retina and are critical for maintenance of the blood-retinal barrier [31]. Müller cells obtain a gliotic phenotype in response to tissue stress and injury that can be visualised by their increased expression of glial fibrillary associated protein (GFAP) [31]. Three μm paraffin sections of retina were incubated overnight at 4 °C

with a rabbit polyclonal anti-GFAP antibody (1:500, Z0334, DakoCytomation, Glostrup, Denmark). The sections were then washed with PBS and incubated for 1 h with Alexa Flour 488-conjugated goat anti-rabbit IgG (1:200, A-11008, Life Technologies, VIC, Australia). The sections were washed with PBS, counterstained with 4',6-diamidino-2-3 phenylindole (DAPI, 0.5 µg/mL, D9542, Molecular Probes, Sigma) and coverslipped with Dako fluorescent mounting medium (S3023, DakoCytomation).

Quantitation of GFAP immunolabelling in retina

The expression of GFAP was quantitated as previously reported [11, 23]. Four sections at least 60 µm apart were randomly selected from one eye from each animal. In each section, 4 non-overlapping fields from the central, mid and peripheral retina that span the entire retina were captured at x400 magnification using a Nikon DS-Ri2 camera (Nikon Instruments Inc. NY, USA). ImageJ software set a threshold for immunolabeling applied to all fields. Data are presented as the percentage of GFAP immunolabelling per field of central, mid, peripheral and whole retina. Investigators were masked to the experimental groups.

ELISA

To further explore damage to the blood-retinal barrier, retinal vascular leakage was measured with an albumin ELISA, and VEGFA protein levels by ELISA in accordance with previous publications [11, 23]. To exclude any contribution of circulating protein from the measurements, mice were perfused via the heart with PBS (5 ml) prior to tissue collection. Retinas were digested in 200 µl of T-PER buffer (Invitrogen, Waltham, MA, USA) containing a phosphatase-protease inhibitor cocktail (1/100, Thermo Fisher Scientific, Victoria, Australia) using a Bullet Blender Tissue Homogenizer (Next Advance, NY, USA) for 5 min at speed 9 at 4 °C. Protein lysates were centrifuged at 10,000 rpm for 10 min at 4 °C and supernatants collected. Samples were run in duplicate for mouse albumin (#E-90AL, Immunology Consultants Laboratory, Portland, OR, USA) and mouse VEGFA (#DY493, R&D Systems, MN, USA) according to the manufacturer's instructions. Total protein concentration of retinal homogenates was measured using a Bradford assay (Biorad). Albumin and VEGFA levels were normalised to the total protein concentration.

Table 1 Body weights of C57BL/6J mouse pups at P12 and P18. HSA, human serum albumin

Mouse groups	P12 Body weight (g)	*n*	P18 Body weight (g)	*n*
Room air control	7.2 ± 0.19	12	8.6 ± 0.14	40
Room air + HSA	NA		8.4 ± 0.15	19
OIR control	5.6 ± 0.06***	10	7.2 ± 0.06***	55
OIR + HSA	NA		7.4 ± 0.07***	25
OIR + AAT	5.9 ± 0.09**	13	7.5 ± 0.07***	61

AAT, alpha-1 antitrypsin. $^{**}p < 0.01$, and $^{***}p < 0.001$ to room air controls. Values are mean ± SEM. $N = 19$ to 61 mice per group from 3 to 4 litters of mice per group. Data were analysed by Kruskal-Wallis test followed by Dunn's test

Statistics

Data were first assessed for normality by Kolmogorov-Smirnov, D'Agostino's and Pearson omnibus, as well as Shapiro-Wilk normality tests. For normally distributed data with equal variances, one-way ANOVA followed by Tukey's post hoc test was used. For normally distributed data with unequal variances, Welch's ANOVA followed by Dunnett's T3 test was used. Non-parametric data were analysed using the Kruskal-Wallis test followed by Dunn's post-test. The sample size was estimated by a power analysis assuming a normal distribution. P-values smaller than 0.05 were considered significant. Investigators were masked to the experimental groups. Values are expressed as mean ± SEM.

Results

Body weight is not influenced by AAT

As expected, OIR controls had reduced body weight at P12 and P18 compared to room air controls. AAT and the protein control, HSA, did not influence the body weight of room air controls or OIR controls (Table 1).

AAT levels are reduced in OIR

Reduced levels of AAT are associated with the development of some diseases [32, 33]. We found in phase I OIR at P12, circulating AAT levels in OIR mice (987.2 ± 28.32 µg/mL) were reduced compared to room air controls (1362 ± 32.68 µg/mL, $p < 0.0001$, $n = 9$ to 13 mice per group). At the end of phase II OIR at P18, circulating AAT levels in OIR mice (1512 ± 44.16 µg/mL) were like room air controls (1685 ± 76.92 µg/mL, $n = 9$ to 13 mice per group).

AAT reduced Iba1 + cell density in phase II OIR

At P18, few Iba1 + cells were identified in room air controls and room air + HSA (Supplemental Fig. 1). In OIR controls and OIR + HSA, the density of Iba1 + cells was similar and increased compared to room air mice (Supplemental Fig. 1). In OIR mice, treatment with AAT reduced the density of Iba1 + cells compared to OIR controls but not to the level of room air controls (Supplemental Fig. 1). Similar results were found in retinal flatmounts, with Iba1 + cells increased in OIR controls and OIR + HSA and often associated with neovascular tufts, compared to room air controls (Fig. 2A). In OIR mice treated with AAT, the number of Iba1 + cells in retinal flatmounts was reduced compared to OIR controls but not to the room air control levels (Fig. 2B).

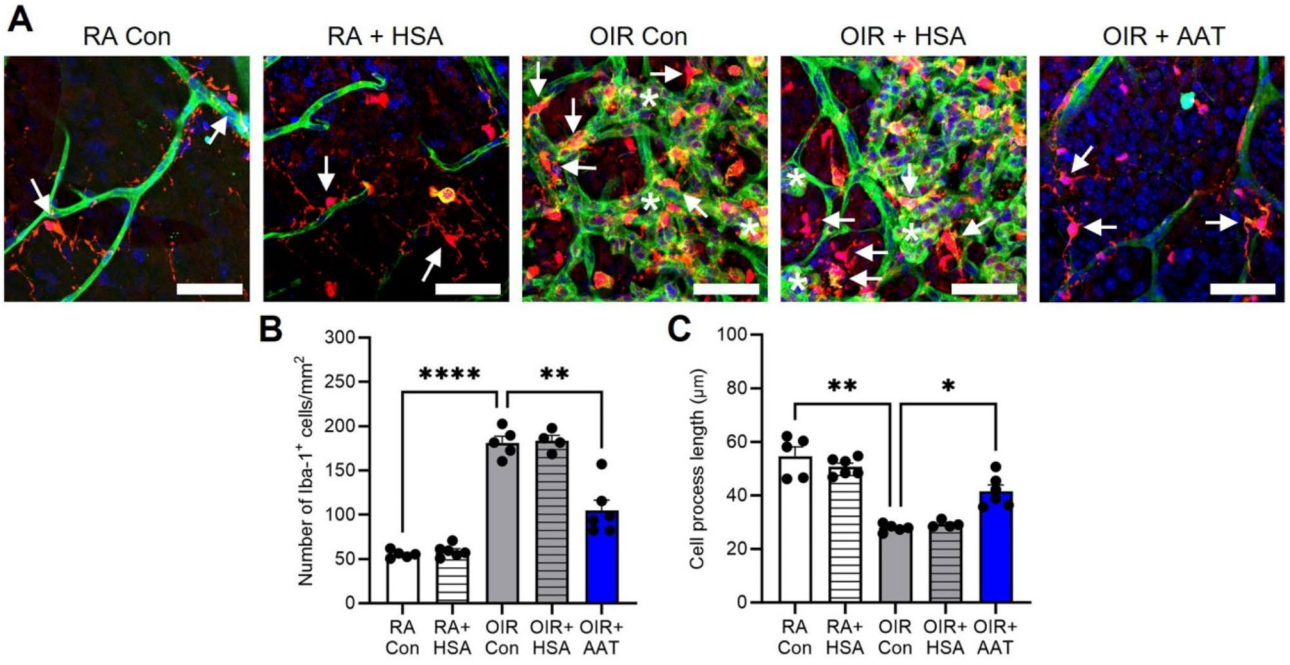

Fig. 2 AAT reduced the number of Iba1 + cells and prevented the reduction in cell process length in phase II OIR mice at P18. RA, room air. Con, control. HSA, human serum albumin, AAT, alpha-1 antitrypsin. **(A)** Representative images of retinal flatmounts labelled with Iba1 showing microglia/macrophages (red, arrows), FITC-isolectin blood vessels (green), and DAPI nuclei (blue). Neovascular tufts are denoted by asterisks. Scale bar, 50 µm. **(B)** Quantitation of Iba1 + cells per mm^2 within the ganglion cell layer and inner plexiform layer. **(C)** Quantitation of the primary cell process length of each $Iba1^+$ cell within the ganglion cell layer and inner plexiform layer. $n = 4$ to 6 mice per group. Values are mean ± SEM. $^*p < 0.05$, $^{**}p < 0.01$, and $^{****}p < 0.0001$. Data were analysed by one-way ANOVA followed by Tukey's test

AAT restored cell process length of Iba1 + cells in phase II OIR

At P18, the cell process length of Iba1 + cells was similar between room air controls and room air + HSA (Fig. 2C). In OIR controls, Iba1 + cells had shorter cell processes compared to room air controls indicating an activated profile (Fig. 2C). In OIR mice treated with AAT, the cell processes of Iba1 + cells were longer compared to OIR controls and resembled room air controls (Fig. 2C).

AAT reduced the number of macrophages in phase II OIR

As Iba1 immunolabelling does not distinguish between microglia and macrophages, flow cytometry of retina was performed. At P18, the density and total cell count of $CD45^{mid}CD11b^+$ microglia and $CD45^{hi}CD11b^+$ macrophages were increased to a similar extent in the retina of OIR controls and OIR + HSA compared to room air controls (Fig. 3A-E). Treatment of OIR mice with AAT reduced macrophages and not microglia in retina (Fig. 3A-E).

Inflammatory factors in phase II OIR

Inflammation is associated with the neovascularization that develops in phase II OIR [34]. We therefore evaluated the expression of pro-inflammatory factors in the retina at P18. The mRNA expression of *Tnf*, *Mcp-1*, *Il-6*, and *Il-1b* were increased in the retina of OIR controls compared to room air controls (Fig. 4A-D). Treatment of OIR mice with AAT reduced the mRNA levels of *Tnf*, and *Mcp-1*, but not *Il-6* and *Il-1b* compared to OIR controls (Fig. 4A-D). In the OIR + AAT group, the mRNA levels of *Il-1b* remained increased compared to room air controls (Fig. 4D).

AAT reduced retinal vaso-obliteration and neovascularisation

In phase I OIR at P18, AAT reduced neovascularisation and vaso-obliteration in retina by almost 50% compared to OIR controls and OIR + HSA (Fig. 5A-C). We next evaluated phase I OIR when retinal vaso-obliteration is maximal. In OIR control mice, retinal vaso-obliteration at P12 was approximately twice as severe than at P18 (Fig. 5B, D). In OIR mice at P12, treatment with AAT treatment reduced retinal vaso-obliteration compared to OIR controls (Fig. 5D).

AAT reduced retinal gliosis, VEGFA and vascular leakage in phase II OIR

GFAP immunolabelling in room air controls and room air + HSA at P18 was similar and confined to the surface of the retina in the region of the inner limiting membrane and ganglion cell layer in the mid, central and peripheral

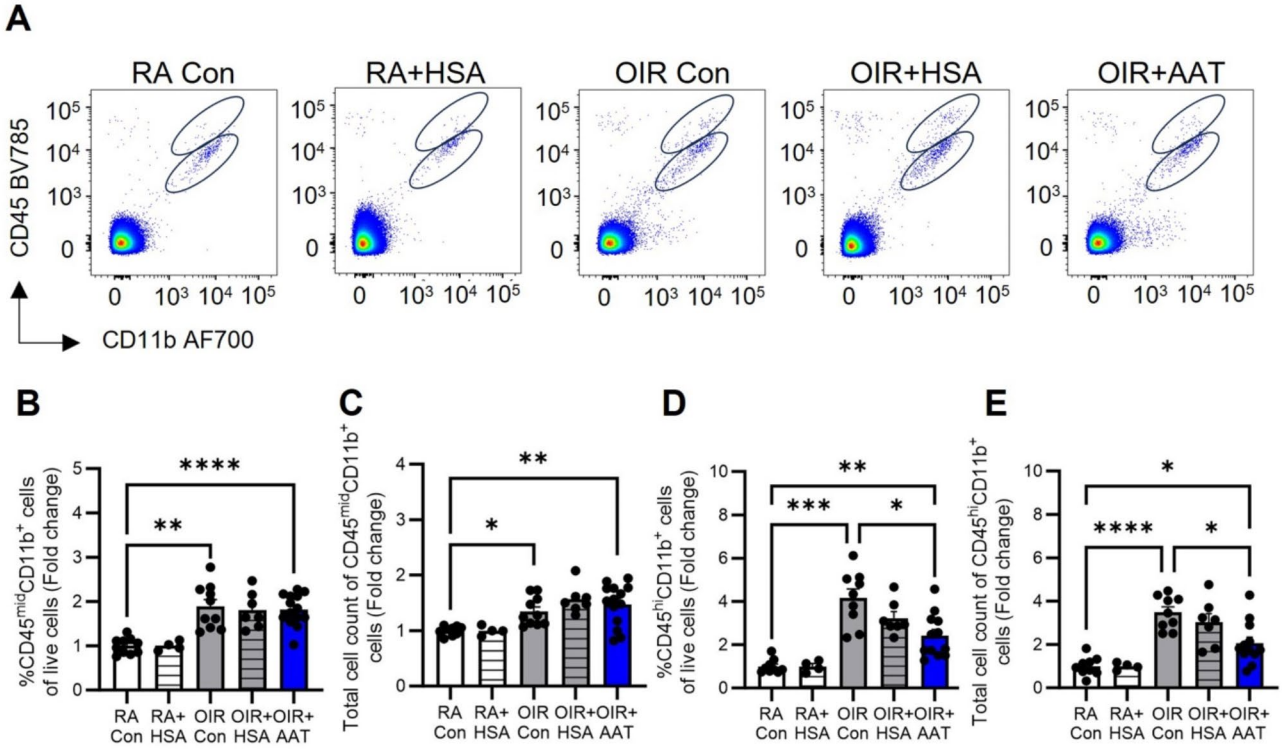

Fig. 3 AAT reduced the number of macrophages in the retina of phase II OIR mice at postnatal day 18. RA, room air. Con, control. HSA, human serum albumin. AAT, alpha-1 antitrypsin. **A.** Gating strategy for $CD45^{mid}CD11b^{+}$ microglia and $CD45^{hi}CD11b^{+}$ macrophages. Fold change in the density (**B**) and total cell count (**C**) of $CD45^{mid}CD11b^{+}$ cells in retina. Fold change in the density (**D**) and total cell count (**E**) of $CD45^{hi}CD11b^{+}$ cells in retina. $n = 4$ to 16 mice per group. Values are mean ± SEM. *$p < 0.05$, **$p < 0.01$, ***$p < 0.001$, and ****$p < 0.0001$. Data were analysed by Welch's ANOVA followed by Dunnett's T3 test

retina (Fig. 6A, B). In OIR controls and OIR + HSA, GFAP immunolabelling was increased to a similar extent compared to room air control mice, extending throughout the retina in Müller cell processes (Fig. 6A, B). In OIR mice, treatment with AAT reduced GFAP immunolabelling in all regions of the retina compared to OIR controls (Fig. 6A, B).

VEGFA can stimulate vascular leakage in the retina [35]. In OIR controls at P18, *Vegfa* mRNA levels in retina were increased compared to room air controls (Fig. 6C). In OIR mice, treatment with AAT reduced *Vegfa* mRNA levels compared to OIR controls (Fig. 6C). VEGFA protein levels and vascular leakage in retina were increased in OIR controls compared to room air controls. In OIR mice both VEGFA protein and vascular leakage in retina were reduced by AAT treatment (Fig. 6D, E).

Discussion

The major findings of this study are that circulating AAT levels are reduced in OIR, and AAT treatment attenuates key aspects of retinal vasculopathy including vaso-obliteration, neovascularisation, gliosis, VEGFA, and vascular leakage. It is yet to be fully understood if AAT directly influences the retinal vasculature and/or protects the vasculature through its anti-gliotic and anti-inflammatory properties as evidenced by reductions in *Tnf* and *Mcp-1* mRNA levels. The source of these inflammatory factors was not investigated, but microglia/macrophages are a possibility with AAT reducing their density in retina.

Inflammation is a major contributor to retinal vascular disease and is mediated by certain cytokines [36–39]. There is considerable evidence that AAT reduces pro-inflammatory molecules such as TNF, MCP-1, IL-6, and IL-1ß [40, 41]. In the current study, AAT reduced the mRNA expression of *Tnf* and *Mcp-1* in the retina in phase II OIR at P18. TNF is a well-known causal factor in the development of retinal vascular disease [11, 36] and therefore AAT's reduction of TNF levels in OIR is noteworthy. With respect to MCP-1, AAT's influence is likely multifaceted, with evidence suggesting that serine proteases like cathepsin G indirectly increase MCP-1 expression and activity through protease-activated receptors and inflammatory mediators [42]. Relevant to OIR are data demonstrating that MCP-1 blocking antibodies reduced retinal neovascularisation [34]. The reason for the inability of AAT to reduce IL-6 and IL-1ß at P18 in OIR is unclear but may relate to the phase of OIR with reports that IL-1ß expression in microglia is particularly elevated in phase I OIR [43].

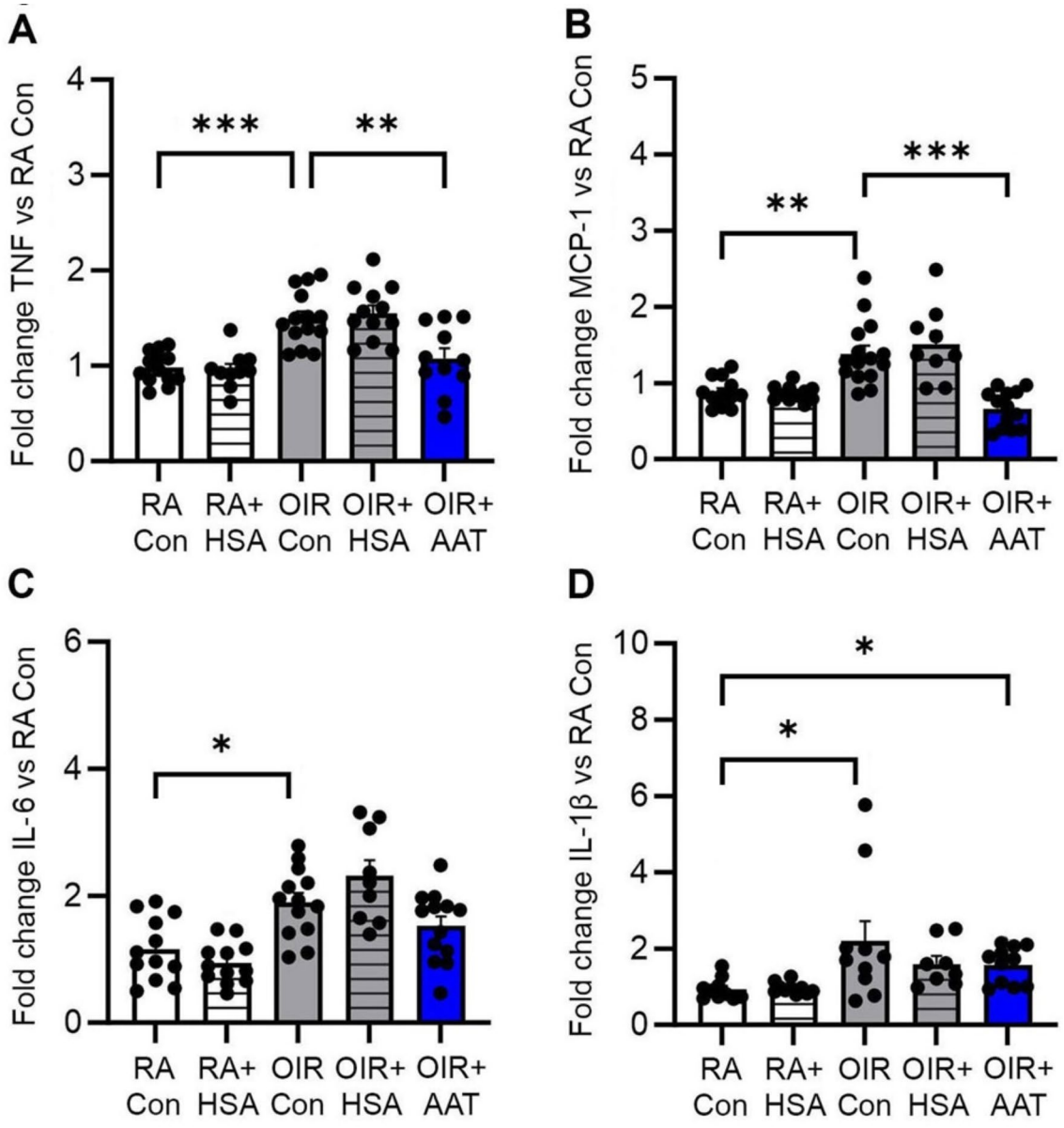

Fig. 4 AAT reduced the expression of *Tnf* and *Mcp-1* in the retina of phase II OIR mice at P18. RA, room air. Con, control. HSA, human serum albumin. AAT, alpha-1 antitrypsin. mRNA levels of (**A**)*Tnf*, (**B**)*Mcp-1*, (**C**)*Il-6*, and (**D**) *Il-1*b. $n = 8$ to 15 mice per group. Values are mean ± SEM. *$p < 0.05$, **$p < 0.01$, and ***$p < 0.001$. Data were analysed using one-way ANOVA followed by Tukey's test or Welch's ANOVA followed by Dunn's test, or the Kruskal-Wallis test followed by Dunn's test

In response to the tissue stress and relative hypoxia that occurs in phase II OIR, microglia undergo distinct cellular changes that result in a pro-inflammatory phenotype [10, 37, 44, 45]. This includes cell proliferation in the inner retina and associated with the vasculature, and cell activation involving their transition from a ramified to ameboid appearance with shorter cell processes and the expression of activation markers [23]. Our morphological analysis of Iba1 + cells revealed that AAT reduced the number of microglia/macrophage cells and partially prevented the phenotypic changes associated with microglial activation, consistent with previous reports in models of ocular hypertension and retinal degeneration showing AAT reducing Iba1 + cells [21, 22]. However, our flow cytometry data revealed a more nuanced response. AAT treatment reduced the number of retinal macrophages ($CD45^{hi}CD11b+$), but not microglia ($CD45^{mid}CD11b+$). This reduction in macrophages suggests that these cells participate in mediating the protective effects of AAT, as they have been shown to promote inflammation and neovascularisation in OIR [46]. An outstanding question is whether the retinal microglia/macrophage population are a source of AAT with previous studies identifying that some microglia/macrophages (positive for Iba1) are

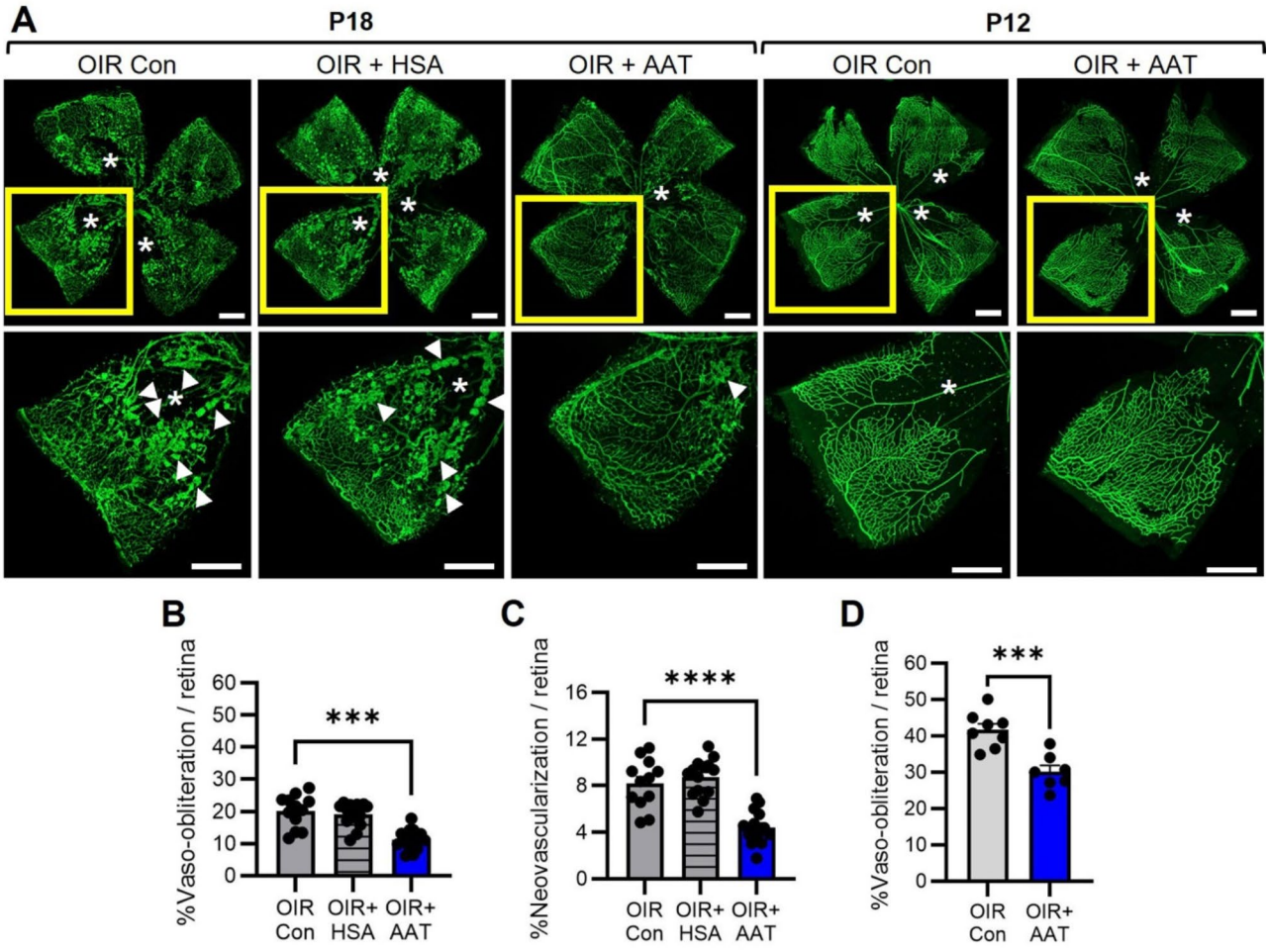

Fig. 5 AAT reduced vascular pathology in retina of OIR mice at P18 and P12. Con, control. HSA, human serum albumin. AAT, alpha-1 antitrypsin. **A**. Representative images of retinal flatmounts stained with FITC-isolectin to show blood vessels (green). Top panels show whole retina. A quadrant of retina (yellow box) is magnified in the lower panel. Asterisks denote vaso-obliteration. Arrowheads denote neovascularisation. Scale bar, 500 µm. **B**. Quantitation of vaso-obliteration at P18. **C.** Quantitation of neovascularisation at P18. **D**. Quantitation of vaso-obliteration at P12. $n = 7$ to 15 mice from 2 to 3 litters of mice per group. ***$p < 0.001$, and ****$p < 0.0001$. Data were analysed using one-way ANOVA followed by Tukey's test or Welch's ANOVA followed by Dunnett's T3 test, or unpaired *t* test. Values are mean ± SEM

immunolabelled for AAT, and AAT expression is reduced in retinal neurodegeneration [22]. Our finding that plasma levels of AAT are reduced in phase I OIR suggests that retinal AAT may in part be derived from the circulation.

Neovascularisation in the inner retina involves the growth of abnormally formed vessels into the vitreous cavity. It is a hallmark feature of retinopathy of prematurity and diabetic retinopathy and is accompanied by the leakage of fluid and protein into the retina and vitreous cavity from a compromised blood-retinal barrier [5, 47]. The OIR model recapitulates many of the features of retinopathy of prematurity but is also used to study the retinal vasculopathy that develops in proliferative diabetic retinopathy, albeit the hyperglycaemia of diabetes is absent [48]. In the current study, we demonstrated that AAT administered at the commencement of phase II OIR, reduced retinal neovascularisation, a finding that to our knowledge has not been previously reported. There is some evidence from other disease models, that AAT influences blood vessel growth such as inhibiting tumour angiogenesis, neovascularisation in the rat cornea and the chemotaxis of human microvascular endothelial cells [49, 50]. Retinal neovascularisation in OIR is influenced by the extent of vaso-obliteration that peaks in phase I as a response to high oxygen exposure that disrupts physiological angiogenesis [47]. AAT's reduction of vaso-obliteration in phase I OIR is therefore important, however the precise mechanisms of action are currently unclear, but could relate to the ability of AAT to suppress endothelial cell apoptosis [51]. Overall, our findings build on previous research in the retina identifying that AAT attenuates neurodegeneration by preventing ganglion cell loss in diabetic animals [20], promotes the survival

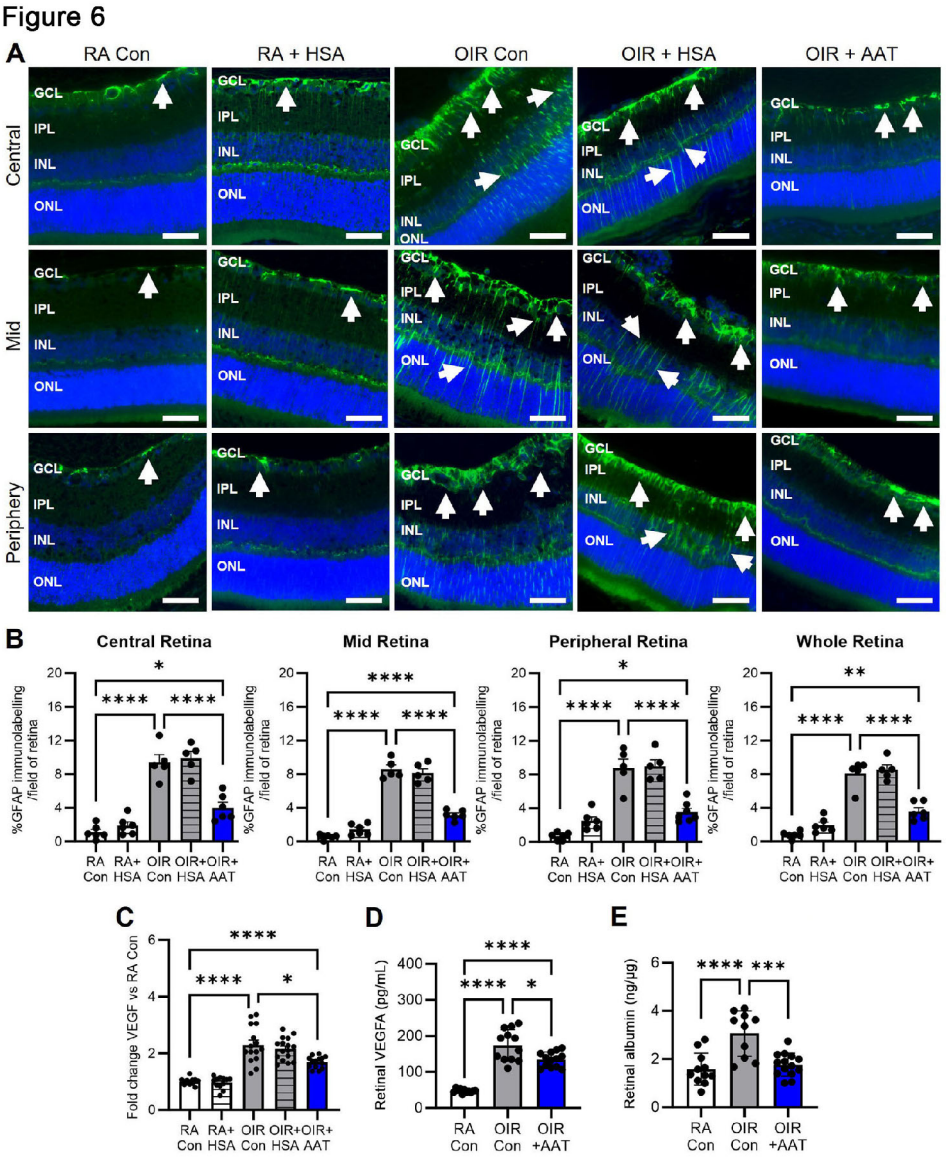

Fig. 6 AAT reduced retinal gliosis, VEGFA, and vascular leakage in phase II OIR mice at P18. RA, room air. Con, control. HSA, human serum albumin. AAT, alpha-1 antitrypsin. **(A)** Representative 3 µm paraffin sections of retina showing GFAP immunolabelling (green) in Müller cell processes (arrows). Nuclei counterstained with DAPI (blue). GCL, ganglion cell layer. IPL, inner plexiform layer. INL, inner nuclear layer. ONL, outer nuclear layer. Scale bar, 50 µm. **(B)** Quantitation of GFAP in the central, mid, peripheral and whole retina by One-way ANOVA. $n = 5$ to 6 mice per group. *$p < 0.05$, **$p < 0.01$, and ****$p < 0.0001$. **C.** *Vegfa* mRNA in retina. **D.** VEGFA protein in retina from mice perfused with PBS. **E.** Retinal vascular leakage (albumin ELISA) in retina from mice perfused with PBS. Values are mean ± SEM. $n = 9$ to 15 mice per group. *$p < 0.05$, ***$p < 0.001$, and ****$p < 0.0001$. Data were analysed by Welch ANOVA followed by Dunnett's T3 tests and one-way ANOVA followed by Tukey's test

of transplanted inducible pluripotent stem cells in mice with ocular hypertension [21], and reduces retinal photoreceptor dysfunction in a mouse model of retinitis pigmentosa [22].

Macroglial Müller cells have an important role in the development of retinal vasculopathy due to their close association with the vasculature [31]. In OIR, Müller cells undergo reactive gliosis in response to the relative tissue hypoxia caused by mice transitioning from a high oxygen environment in phase I OIR to room air in phase II OIR. Accompanying this gliotic phenotype is the increased production of VEGFA by Müller cells which stimulates retinal neovascularisation and vascular permeability [3, 4]. In the current study, AAT treatment during phase II OIR reduced Müller cell gliosis in the central, mid and peripheral regions, and elevated VEGFA mRNA and protein levels in the retina. If AAT directly influences VEGFA expression and secretion is not fully understood. However, it has been suggested that in diabetic retinopathy certain metalloproteinases involved in regulation of

the extracellular matrix and vascular basement membrane thickening are inhibited by AAT, resulting in reduced VEGFA levels and potentially vasculopathy [52, 53]. In terms of our finding that AAT reduced vascular permeability in the OIR retina, these results are consistent with reports that AAT protected the immature mouse brain from hypoxic injury including breakdown of the blood-brain barrier [54].

Conclusions

The findings of this study indicate that AAT can protect the retinal vasculature against vision threatening disease. Our finding that AAT levels are reduced in the circulation of mice in phase I OIR are in agreement with studies in patients with diabetic retinopathy showing reduced AAT levels [32, 33] and activity [55]. Evidence that AAT augmentation is beneficial in diabetic models [56, 57] and in our study of OIR suggests that AAT is a potential treatment approach for these neovascular retinopathies.

Abbreviations

Alpha-1	Antitrypsin AAT
DAPI	4′,6-diamidino-2-3 phenylindole
FITC	Fluorescein isothiocyanate
GFAP	Glial fibrillary acidic protein
HSA	Human serum albumin
Iba1	Ionised binding adaptor protein 1
IL	Interleukin
IP	Intraperitoneal
MCP-1	Monocyte chemoattractant protein 1
MFI	Mean fluorescent intensity
OIR	Oxygen-induced retinopathy
P	Postnatal day
PBS	Phosphate buffered saline
PCR	Polymerase chain reaction
TNF	Tumour necrosis factor
VEGFA	Vascular endothelial growth factorA

Supplementary Information

The online version contains supplementary material available at https://doi.org/10.1186/s12950-025-00431-3.

Supplementary Material 1

Acknowledgements

The authors thank the Biological Optical Microscopy Platform at the University of Melbourne for expert imaging advice.

Author contributions

Y-HL, SP, AK, CH, ABM, DD and JW-B conceived and designed the experiments. VS and AJ performed the experiments and collected the data. VS and DD analysed the data. JW-B wrote the manuscript. All authors revised and approved the final manuscript. All authors accept responsibility for the accuracy of the content of the final manuscript.

Funding

This research was supported by a grant from CSL Limited (Parkville, Victoria, Australia).

Data availability

The datasets used and/or analysed during the current study are available from the corresponding author on reasonable request.

Declarations

Ethics approval and consent to participate

The study was granted ethical approval by the University of Melbourne Animal Ethics Committee (number: 10452).

Consent for publication

Not applicable.

Competing interests

The competing interests are as follows. JW-B received funding from CSL Limited (Parkville, Victoria, Australia) to undertake the study. Y-HL, SP, AK, CH, and ABM are employees of CSL Limited.

Received: 12 August 2024 / Accepted: 27 January 2025
Published online: 11 February 2025

References

1. Blencowe H, Lawn JE, Vazquez T, Fielder A, Gilbert C. Preterm-associated visual impairment and estimates of retinopathy of prematurity at regional and global levels for 2010. Pediatr Res. 2013;74(Suppl 1):35–49.
2. Cho NH, Shaw JE, Karuranga S, Huang Y, da Rocha Fernandes JD, Ohlrogge AW, Malanda B. IDF Diabetes Atlas: global estimates of diabetes prevalence for 2017 and projections for 2045. Diabetes Res Clin Pract. 2018;138:271–81.
3. Bai Y, Ma JX, Guo J, Wang J, Zhu M, Chen Y, Le YZ. Muller cell-derived VEGF is a significant contributor to retinal neovascularization. J Pathol. 2009;219:446–54.
4. Pierce EA, Avery RL, Foley ED, Aiello LP, Smith LE. Vascular endothelial growth factor/vascular permeability factor expression in a mouse model of retinal neovascularization. Proc Natl Acad Sci U S A. 1995;92:905–9.
5. Simo R, Hernandez C. Novel approaches for treating diabetic retinopathy based on recent pathogenic evidence. Prog Retin Eye Res. 2015;48:160–80.
6. Bahr TA, Bakri SJ. Update on the management of Diabetic Retinopathy: Anti-VEGF agents for the Prevention of complications and Progression of Nonproliferative and proliferative retinopathy. Life (Basel) 2023; 13.
7. Taher NO, Ghaddaf AA, Al-Ghamdi SA, Homsi JJ, Al-Harbi BJ, Alomari LK, Almarzouki HS. Intravitreal anti-vascular endothelial growth factor injection for retinopathy of Prematurity: a systematic review and Meta-analysis. Front Med (Lausanne). 2022;9:884608.
8. Enriquez AB, Avery RL, Baumal CR. Update on anti-vascular endothelial growth factor safety for retinopathy of Prematurity. Asia Pac J Ophthalmol (Phila). 2020;9:358–68.
9. Nitkin CR, Bamat NA, Lagatta J, DeMauro SB, Lee HC, Patel RM, King B, Slaughter JL, Campbell JP, Richardson T, Lewis T. Pulmonary hypertension in Preterm infants treated with laser vs anti-vascular endothelial growth factor therapy for retinopathy of Prematurity. JAMA Ophthalmol. 2022;140:1085–94.
10. Kinuthia UM, Wolf A, Langmann T. Microglia and inflammatory responses in Diabetic Retinopathy. Front Immunol. 2020;11:564077.
11. Deliyanti D, Figgett WA, Gebhardt T, Trapani JA, Mackay F, Wilkinson-Berka JL. CD8(+) T cells promote pathological angiogenesis in Ocular Neovascular Disease. Arterioscler Thromb Vasc Biol. 2023;43:522–36.
12. Gao X, Wang YS, Li XQ, Hou HY, Su JB, Yao LB, Zhang J. Macrophages promote vasculogenesis of retinal neovascularization in an oxygen-induced retinopathy model in mice. Cell Tissue Res. 2016;364:599–610.
13. Janciauskiene S, Wrenger S, Immenschuh S, Olejnicka B, Greulich T, Welte T, Chorostowska-Wynimko J. The Multifaceted effects of Alpha1-Antitrypsin on Neutrophil functions. Front Pharmacol. 2018;9:341.
14. O'Brien ME, Murray G, Gogoi D, Yusuf A, McCarthy C, Wormald MR, Casey M, Gabillard-Lefort C, McElvaney NG, Reeves EP. A review of Alpha-1 antitrypsin binding partners for Immune Regulation and potential therapeutic application. Int J Mol Sci 2022; 23.
15. Hunt JM, Tuder R. Alpha 1 anti-trypsin: one protein, many functions. Curr Mol Med. 2012;12:827–35.
16. McElvaney OF, Fraughen DD, McElvaney OJ, Carroll TP, McElvaney NG. Alpha-1 antitrypsin deficiency: current therapy and emerging targets. Expert Rev Respir Med. 2023;17:191–202.
17. Shahaf G, Moser H, Ozeri E, Mizrahi M, Abecassis A, Lewis EC. Alpha-1-antitrypsin gene delivery reduces inflammation, increases T-regulatory cell population size and prevents islet allograft rejection. Mol Med. 2011;17:1000–11.

18. Subramanian S, Shahaf G, Ozeri E, Miller LM, Vandenbark AA, Lewis EC, Offner H. Sustained expression of circulating human alpha-1 antitrypsin reduces inflammation, increases CD4 + FoxP3 + Treg cell population and prevents signs of experimental autoimmune encephalomyelitis in mice. Metab Brain Dis. 2011;26:107–13.
19. Koulmanda M, Bhasin M, Hoffman L, Fan Z, Qipo A, Shi H, Bonner-Weir S, Putheti P, Degauque N, Libermann TA, et al. Curative and beta cell regenerative effects of alpha1-antitrypsin treatment in autoimmune diabetic NOD mice. Proc Natl Acad Sci U S A. 2008;105:16242–7.
20. Ortiz G, Lopez ES, Salica JP, Potilinski C, Fernandez Acquier M, Chuluyan E, Gallo JE. Alpha-1-antitrypsin ameliorates inflammation and neurodegeneration in the diabetic mouse retina. Exp Eye Res. 2018;174:29–39.
21. Yang S, Xian B, Li K, Luo Z, Liu Y, Hu D, Ge J. Alpha 1-antitrypsin inhibits microglia activation and facilitates the survival of iPSC grafts in hypertension mouse model. Cell Immunol. 2018;328:49–57.
22. Zhou T, Huang Z, Zhu X, Sun X, Liu Y, Cheng B, Li M, Liu Y, He C, Liu X. Alpha-1 Antitrypsin attenuates M1 microglia-mediated neuroinflammation in Retinal Degeneration. Front Immunol. 2018;9:1202.
23. Deliyanti D, Talia DM, Zhu T, Maxwell MJ, Agrotis A, Jerome JR, Hargreaves EM, Gerondakis S, Hibbs ML, Mackay F, Wilkinson-Berka JL. Foxp3(+) tregs are recruited to the retina to repair pathological angiogenesis. Nat Commun. 2017;8:748.
24. Smith LE, Wesolowski E, McLellan A, Kostyk SK, D'Amato R, Sullivan R, D'Amore PA. Oxygen-induced retinopathy in the mouse. Invest Ophthalmol Vis Sci. 1994;35:101–11.
25. Pierce EA, Foley ED, Smith LE. Regulation of vascular endothelial growth factor by oxygen in a model of retinopathy of prematurity. Arch Ophthalmol. 1996;114:1219–28.
26. Higgins RD, Yan Y, Tadesse M, Yossuck P. Lack of effect of gender on retinopathy in the mouse. Clin Exp Ophthalmol. 2001;29:323–6.
27. Boeck M, Thien A, Wolf J, Hagemeyer N, Laich Y, Yusuf D, Backofen R, Zhang P, Boneva S, Stahl A, et al. Temporospatial distribution and transcriptional profile of retinal microglia in the oxygen-induced retinopathy mouse model. Glia. 2020;68:1859–73.
28. Deliyanti D, Miller AG, Tan G, Binger KJ, Samson AL, Wilkinson-Berka JL. Neovascularization is attenuated with aldosterone synthase inhibition in rats with retinopathy. Hypertension. 2012;59:607–13.
29. Deliyanti D, Armani R, Casely D, Figgett WA, Agrotis A, Wilkinson-Berka JL. Retinal vasculopathy is reduced by dietary salt restriction: involvement of Glia, ENaCalpha, and the renin-angiotensin-aldosterone system. Arterioscler Thromb Vasc Biol. 2014;34:2033–41.
30. McCarthy CA, Widdop RE, Deliyanti D, Wilkinson-Berka JL. Brain and retinal microglia in health and disease: an unrecognized target of the renin-angiotensin system. Clin Exp Pharmacol Physiol. 2013;40:571–9.
31. Bringmann A, Pannicke T, Grosche J, Francke M, Wiedemann P, Skatchkov SN, Osborne NN, Reichenbach A. Muller cells in the healthy and diseased retina. Prog Retin Eye Res. 2006;25:397–424.
32. Sandler M, Gemperli BM, Hanekom C, Kuhn SH. Serum alpha 1-protease inhibitor in diabetes mellitus: reduced concentration and impaired activity. Diabetes Res Clin Pract. 1988;5:249–55.
33. Sandstrom CS, Ohlsson B, Melander O, Westin U, Mahadeva R, Janciauskiene S. An association between type 2 diabetes and alpha-antitrypsin deficiency. Diabet Med. 2008;25:1370–3.
34. Yoshida S, Yoshida A, Ishibashi T, Elner SG, Elner VM. Role of MCP-1 and MIP-1alpha in retinal neovascularization during postischemic inflammation in a mouse model of retinal neovascularization. J Leukoc Biol. 2003;73:137–44.
35. Kumar R, Rottner K, Rao GN. Requirement of Site-Specific Tyrosine Phosphorylation of Cortactin in retinal neovascularization and vascular leakage. Arterioscler Thromb Vasc Biol; 2023.
36. Gardiner TA, Gibson DS, de Gooyer TE, de la Cruz VF, McDonald DM, Stitt AW. Inhibition of tumor necrosis factor-alpha improves physiological angiogenesis and reduces pathological neovascularization in ischemic retinopathy. Am J Pathol. 2005;166:637–44.
37. Talia DM, Deliyanti D, Agrotis A, Wilkinson-Berka JL. Inhibition of the Nuclear receptor RORgamma and Interleukin-17A suppresses Neovascular Retinopathy: involvement of Immunocompetent Microglia. Arterioscler Thromb Vasc Biol. 2016;36:1186–96.
38. Fuchs H, Chen LZ, Low S, Yu H. Ocular and systemic pharmacokinetics of BI-X, a nanobody targeting VEGF and Ang-2, after intravitreal dosing in cynomolgus monkeys - evidence for half-life extension by albumin. Exp Eye Res. 2021;205:108486.
39. Wooff Y, Man SM, Aggio-Bruce R, Natoli R, Fernando N. IL-1 family members mediate cell death, inflammation and angiogenesis in retinal degenerative diseases. Front Immunol. 2019;10:1618.
40. Janciauskiene S, Larsson S, Larsson P, Virtala R, Jansson L, Stevens T. Inhibition of lipopolysaccharide-mediated human monocyte activation, in vitro, by alpha1-antitrypsin. Biochem Biophys Res Commun. 2004;321:592–600.
41. Schuster R, Motola-Kalay N, Baranovski BM, Bar L, Tov N, Stein M, Lewis EC, Ayalon M, Sagiv Y. Distinct anti-inflammatory properties of alpha1-antitrypsin and corticosteroids reveal unique underlying mechanisms of action. Cell Immunol. 2020;356:104177.
42. Sharony R, Yu PJ, Park J, Galloway AC, Mignatti P, Pintucci G. Protein targets of inflammatory serine proteases and cardiovascular disease. J Inflamm (Lond). 2010;7:45.
43. Rivera JC, Sitaras N, Noueihed B, Hamel D, Madaan A, Zhou T, Honore JC, Quiniou C, Joyal JS, Hardy P, et al. Microglia and interleukin-1beta in ischemic retinopathy elicit microvascular degeneration through neuronal semaphorin-3A. Arterioscler Thromb Vasc Biol. 2013;33:1881–91.
44. Fu X, Feng S, Qin H, Yan L, Zheng C, Yao K. Microglia: the breakthrough to treat neovascularization and repair blood-retinal barrier in retinopathy. Front Mol Neurosci. 2023;16:1100254.
45. Rana I, Suphapimol V, Jerome JR, Talia DM, Deliyanti D, Wilkinson-Berka JL. Angiotensin II and aldosterone activate retinal microglia. Exp Eye Res. 2020;191:107902.
46. Zhou Y, Yoshida S, Nakao S, Yoshimura T, Kobayashi Y, Nakama T, Kubo Y, Miyawaki K, Yamaguchi M, Ishikawa K, et al. M2 macrophages enhance pathological neovascularization in the mouse model of Oxygen-Induced Retinopathy. Invest Ophthalmol Vis Sci. 2015;56:4767–77.
47. Sapieha P, Joyal JS, Rivera JC, Kermorvant-Duchemin E, Sennlaub F, Hardy P, Lachapelle P, Chemtob S. Retinopathy of prematurity: understanding ischemic retinal vasculopathies at an extreme of life. J Clin Invest. 2010;120:3022–32.
48. Quiroz J, Yazdanyar A. Animal models of diabetic retinopathy. Ann Transl Med. 2021;9:1272.
49. Gacche RN. Changing landscape of anti-angiogenic therapy: novel approaches and clinical perspectives. Biochim Biophys Acta Rev Cancer. 2023;1878:189020.
50. Huang H, Campbell SC, Nelius T, Bedford DF, Veliceasa D, Bouck NP, Volpert OV. Alpha1-antitrypsin inhibits angiogenesis and tumor growth. Int J Cancer. 2004;112:1042–8.
51. Feng Y, Hu L, Xu Q, Yuan H, Ba L, He Y, Che H. Cytoprotective role of Alpha-1 antitrypsin in vascular endothelial cell under Hypoxia/Reoxygenation Condition. J Cardiovasc Pharmacol. 2015;66:96–107.
52. Ortiz G, Salica JP, Chuluyan EH, Gallo JE. Diabetic retinopathy: could the alpha-1 antitrypsin be a therapeutic option? Biol Res. 2014;47:58.
53. Roy S, Bae E, Amin S, Kim D. Extracellular matrix, gap junctions, and retinal vascular homeostasis in diabetic retinopathy. Exp Eye Res. 2015;133:58–68.
54. Zhang S, Li W, Xu Y, Li T, Ek J, Zhang X, Wang Y, Song J, Zhu C, Wang X. Alpha1-antitrypsin protects the immature mouse brain following hypoxic-ischemic injury. Front Cell Neurosci. 2023;17:1137497.
55. Hashemi M, Naderi M, Rashidi H, Ghavami S. Impaired activity of serum alpha-1-antitrypsin in diabetes mellitus. Diabetes Res Clin Pract. 2007;75:246–8.
56. Park SS, Rodriguez Ortega R, Agudelo CW, Perez Perez J, Perez Gandara B, Garcia-Arcos I, McCarthy C, Geraghty P. Therapeutic potential of Alpha-1 antitrypsin in type 1 and type 2 diabetes Mellitus. Medicina (Kaunas) 2021; 57.
57. Song S, Goudy K, Campbell-Thompson M, Wasserfall C, Scott-Jorgensen M, Wang J, Tang Q, Crawford JM, Ellis TM, Atkinson MA, Flotte TR. Recombinant adeno-associated virus-mediated alpha-1 antitrypsin gene therapy prevents type I diabetes in NOD mice. Gene Ther. 2004;11:181–6.

Publisher's note